ARTICLE

The splicing factor WBP11 mediates MCM7 intron retention to promote the malignant progression of ovarian cancer

Yuan Wei[1], Zhongshao Chen[1], Yingwei Li[2]✉ and Kun Song[1]✉

Accumulating studies suggest that splicing factors play important roles in many diseases including human cancers. Our study revealed that WBP11, a core splicing factor, is highly expressed in ovarian cancer (OC) tissues and associated with a poor prognosis. WBP11 inhibition significantly impaired the proliferation and mobility of ovarian cancer cells in vitro and in vivo. Furthermore, FOXM1 transcriptionally activated WBP11 expression by directly binding to its promoter in OC cells. Importantly, RNA-seq and alternative splicing event analysis revealed that WBP11 silencing decreased the expression of MCM7 by regulating intron 4 retention. MCM7 inhibition attenuated the increase in malignant behaviors of WBP11-overexpressing OC cells. Overall, WBP11 was identified as an oncogenic splicing factor that contributes to malignant progression by repressing intron 4 retention of MCM7 in OC cells. Thus, WBP11 is an oncogenic splicing factor with potential therapeutic and prognostic implications in OC.

Oncogene; https://doi.org/10.1038/s41388-024-03015-2

INTRODUCTION

OC ranks first in case-fatality rate among gynecologic malignancies [1]. Most ovarian cancers present at an advanced stage because of the asymptomatic nature of the early stage, and the 5-year survival rate of patients with stage III-IV disease is only 30% [2]. Although OC patients generally accept standard treatment, including debulking surgery and platinum-based chemotherapy, nearly all women will eventually experience recurrence [3]. Therefore, it is urgent to identify and develop novel treatment strategies for OC patients.

Alternative splicing (AS) is a ubiquitous regulatory mechanism that enables cells to generate different RNA variants that encode distinct protein isoforms from a limited number of genes [4]. According to genome-wide studies, it is estimated that more than 90% of human genes express transcript variants [5]. Aberrant splicing is associated with various human diseases, including cancers [6].

WBP11 is recognized as a pre-mRNA splicing factor and colocalizes with SC35 in nuclear speckles [7], the site for splicing factor storage and modification [8]. Studies have shown that it is associated with the PRP19 spliceosome complex [9], a highly dynamic ribonucleoprotein (RNP) machine that removes noncoding introns from precursor messenger RNAs [10]. WBP11 is reported to serve as an endogenous partner of PQBP1, and aberrant gene functions of WBP11 are related to congenital defects and malformation [11, 12]. WBP11 is required in centriole duplication by splicing the TUBGCP6 pre-mRNA [13]. WBP11 promotes the malignant behavior of gastric cancer cells [14]. However, the role of WBP11 in OC has never been reported.

Here, we uncovered that WBP11 is frequently overexpressed in OC and that high expression of WBP11 is associated with a worse prognosis. Furthermore, the functional roles of WBP11 were characterized by in vitro and in vivo assays, and the results showed that WBP11 promoted the malignant behavior of OC cells. Mechanistically, FOXM1 transcriptional activation contributed to high expression of WBP11 in OC cells. Moreover, we provided evidence that WBP11 facilitates the efficient splicing of MCM7. Taken together, these results suggest that WBP11 might be a prognostic indicator and potential treatment target for OC patients.

RESULTS

WBP11 is upregulated in OC and indicates a poor prognosis

To investigate whether splicing factors are involved in the initiation and development of OC, we performed integrated analysis of 4438 upregulated genes from the GEPIA2.0 database, 3864 differentially expressed proteins from the Clinical Proteomic Tumor Analysis Consortium (CPTAC), and 134 core splicing factors from Tiffany's study (Fig. 1A). The results revealed 15 critical splicing factors that might be involved in the evolution of ovarian cancer. Figure 1B demonstrates the expression of 15 splicing factors in high grade serous carcinoma (HGSOC) tissues compared to fallopian tube (FT) and normal ovary tissues. WBP11 was reported to serve as a pre-mRNA splicing factor and was required for centriole duplication, which is closed associated with cell proliferation. Proliferation is an important property of tumor cells, and we focused our attention on WBP11 for further study. We analyzed WBP11 mRNA expression in TCGA and GTEx databases, and the results revealed that it was significantly upregulated in most OC samples compared with normal ovary tissues. There was no significant difference between OC samples and FT samples

[1]Department of Obstetrics and Gynecology, Qilu Hospital of Shandong University, 107 Wenhua Xi Road, Ji'nan 250012 Shandong, China. [2]Department of Obstetrics and Gynecology, Qilu Hospital of Shandong University, Medical Integration and Practice Center, Cheeloo College of Medicine, Shandong University, Ji'nan 250012 Shandong, China. ✉email: sduliyingwei@126.com; songkun2001226@sdu.edu.cn

Received: 25 August 2023 Revised: 20 March 2024 Accepted: 21 March 2024
Published online: 01 April 2024

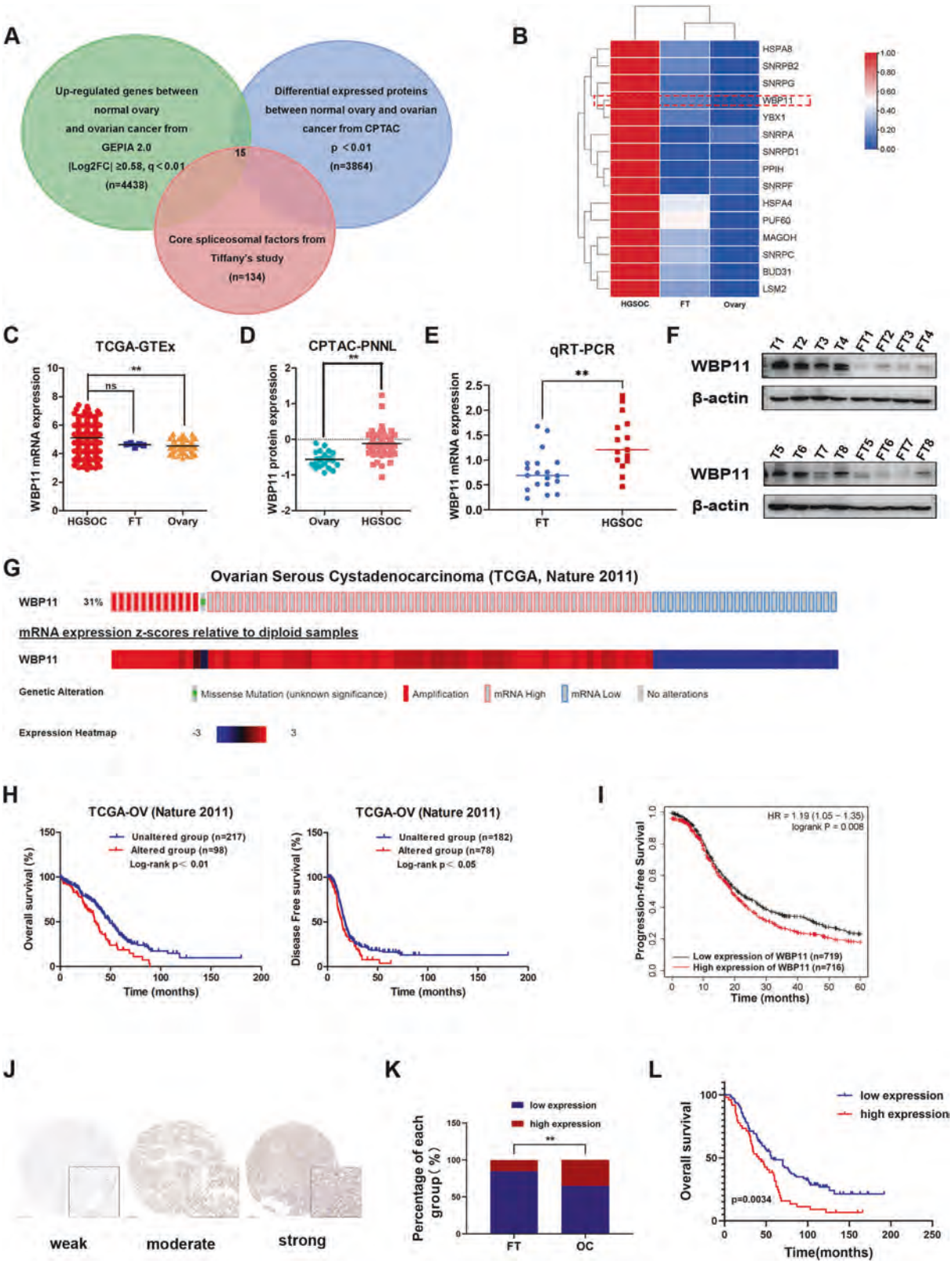

owing to the limited number of FT samples (Fig. 1C). Consistently, WBP11 protein expression was markedly higher in OC tissues than in normal ovary samples according to data from the CPTAC database (Fig. 1D). qRT–PCR and western blotting were used to investigate the differential expression of WBP11 in fresh frozen OC, FT tissues and normal ovaries (OV), and the results showed that WBP11 expression was increased in OC tissues compared with normal FT tissues and OV tissues (Fig. 1E, F, Supplementary Fig. S2A, S1A, B). Moreover, genomic amplification of WBP11 was present in 31% of OC patients in the TCGA cohort (Fig. 1G), and

Fig. 1 WBP11 is upregulated in OC and indicates poor prognosis. A Venn diagram showing 4438 upregulated genes from the GEPIA 2.0 database, 3864 differentially expressed proteins from CPTAC database, and 134 core splicing factors from Tiffany's study. **B** Heat map showing expression levels of 15 splicing factors upregulated in high-grade serous ovarian cancer (HGSOC) ($n = 426$) compared with FTs ($n = 5$) and normal ovary tissues ($n = 88$) from TCGA-GTEx. **C** Relative mRNA expression of WBP11 in ovarian cancer ($n = 426$), normal ovary ($n = 88$) and fallopian tube ($n = 5$) tissues from TCGA-GTEx. **D** Relative protein expression of WBP11 in ovarian cancer ($n = 84$) and normal ovary ($n = 19$) tissues from CPTAC-PNNL. **E** WBP11 mRNA expression between frozen ovarian cancer ($n = 15$) and fallopian tube ($n = 19$) tissues through qRT-PCR. **F** Western blotting of WBP11 protein between ovarian cancer ($n = 8$) and fallopian tube ($n = 8$) tissues. **G** Genetic alterations of WBP11 in ovarian cancer in the cohort from CBioPortal ($n = 316$). **H** Kaplan–Meier analysis showed the effect of WBP11 expression on the overall survival and disease-free survival of ovarian cancer patients from CBioPortal. **I** Kaplan–Meier analysis showed the effect of WBP11 expression on the progression-free survival (High expression group, $n = 716$; Low expression group, $n = 719$) of ovarian cancer patients from Kaplan–Meier Plotter (http://kmplot.com/). **J** Immunohistochemical (IHC) staining images of WBP11 in fallopian tube ($n = 74$) and ovarian cancer ($n = 194$) based the Tissue Microarray of ovarian cancer from our tissue bank. **K** Statistical analysis of WBP11 expression from IHC staining of our tissue microarray. **L** Kaplan–Meier analysis showed the effect of WBP11 expression on the overall survival based the Tissue Microarray of HGSOC from our tissue bank. *P* value was obtained by Log-rank test (**H**, **I**, **L**) or Unpaired t-test (**C**–**E**, **K**). $^{**}P < 0.01$.

WBP11 amplification contributed to its high expression. To obtain further insight into the prognostic significance of WBP11 in OC patients, survival data was retrieved from the public database for analysis. High expression of WBP11 indicated poor overall survival (OS) and disease-free survival (DFS) in the TCGA cohort (Fig. 1H). High expression of WBP11 was also found to be negatively correlated with poor progression-free survival (PFS) using the KM-plotter database (Fig. 1I). In addition, we performed an immunohistochemistry staining assay to assess WBP11 expression in formalin-fixed paraffin-embedded OC tissue ($n = 194$) and normal FT tissues ($n = 74$) based on a tissue microarray (TMA). WBP11 staining was predominantly observed in the nucleus, and a higher level of WBP11 expression was detected in OC samples than in FT samples (Fig. 1J, K). The proportion of samples with high WBP11 expression was 34.97% in the OC group and only 15.07% in the FT group. Then, WBP11 expression was evaluated for its prognostic value in OC patients using our cohort, and we found that the survival time of the high WBP11 expression group was significantly shorter than that of the low expression group, and high expression of WBP11 indicated worse OS (Fig. 1L). Taken together, these results indicate that WBP11 is overexpressed in OC and that high expression of WBP11 indicates a worse prognosis. Thus, WBP11 is a potential prognostic biomarker and treatment target for OC patients.

WBP11 facilitates the proliferation and metastasis of OC cells in vitro

To determine the biological roles of WBP11 in OC cells, WBP11 siRNAs were designed and transiently transfected into HEY, SKOV3 and OVCAR8 cells to suppress WBP11 expression. WBP11-overexpressing OVCAR8 cells were constructed by lentivirus infection. The expression efficiency of WBP11 was validated by qRT–PCR and western blotting (Fig. 2A, B, Supplementary Fig. S2B). CCK-8 growth curves and clonogenic assays were used to investigate the effect of WBP11 expression on the proliferation ability of OC cells, and the results revealed that WBP11 overexpression accelerated the growth of OC cells, whereas WBP11 inhibition slowed the growth of OC cells (Fig. 2C). Consistent with this, WBP11 overexpression further increased the clonogenic capacity, and WBP11 silencing led to a drastic decrease in colony number (Fig. 2D). In addition, the effect of WBP11 on the migratory potential of OC cells was assessed by Transwell migration and Matrigel invasion assays. WBP11 knockdown suppressed the migration and invasion of ovarian cancer cells. In contrast, WBP11 overexpression yielded opposite effects (Fig. 2E). Collectively, these data indicate that WBP11 contributes to OC proliferation and mobility in vitro.

WBP11 promotes tumorigenic ability in vivo

To validate our in vitro findings and assess the ability of WBP11 to promote tumor progression in OC cells in vivo, OVCAR8 cells with WBP11 knockdown (sh-WBP11) and corresponding control cells (sh-NC) were subcutaneously injected into nude mice ($n = 10$). The mice were housed under SPF conditions for 3 weeks. When the mice were killed, the tumors were obtained from the mice (Fig. 3A). The volume and weight of tumors from the WBP11 knockdown group were much lower than those from the control group (Fig. 3B, C). Then, we examined WBP11 and Ki-67 expression in the tumors through immunohistochemistry staining. The results showed that WBP11 and Ki-67 expression was obviously down-regulated in the sh-WBP11 group compared with the control group (Fig. 3D–F). Next, OVCAR8 cells with WBP11 overexpression (PCMV-WBP11) and corresponding control cells (PCMV-NC) were subcutaneously injected into nude mice ($n = 12$). As expected, forced expression of WBP11 in OVCAR8 cells induced a significant increase in tumor mass and volume (Fig. 3G–I). Therefore, these results suggest that WBP11 exhibits oncogenic progression of ovarian cancer.

FOXM1 transcriptionally activates WBP11 expression in OC cells

WBP11 is highly expressed in OC tissues, and the molecular mechanism underlying WBP11 overexpression is unclear. We investigated the transcription factors that could bind to the promoter of WBP11 using CistromeDB, and coexpression analysis of WBP11 was conducted using TCGA OC data from the cBioPortal website. Only FOXM1 was identified through integrated analysis of transcription factors (regulatory potential ≥0.4) and coexpressed genes (Pearson $r \geq 0.4$) (Fig. 4A). The correlation coefficient between FOXM1 and WBP11 was 0.434 (Fig. 4B). Next, we examined whether FOXM1 directly regulates the transcription of WBP11. We first measured the expression of WBP11 after FOXM1 knockdown in OC cells, and we found that FOXM1 inhibition was accompanied by a decrease in the mRNA and protein levels of WBP11 (Fig. 4C, D, Supplementary Fig. S2C). Next, we measured the mRNA expression of FOXM1 after WBP11 knockdown in OC cells. Results showed that mRNA level of FOXM1 is unchanged upon WBP11 knockdown (Supplementary Fig. S1C). Data from the Cistrome Data Browser database showed that FOXM1 binding sites enriched in the promoter regions of WBP11 in multiple cell lines (Fig. 4E). Furthermore, we constructed wild-type (WT) and mutant-type (MT) reporter plasmids of the WBP11 promoter using the pGL4.26 vector. The results of the dual-luciferase reporter assay showed that forced expression of FOXM1 resulted in a 2-fold increase in the luciferase activity of the wild-type reporter plasmid of WBP11 but not the MT plasmid in HEK293T cells (Fig. 4F). Subsequently, chromatin immunoprecipitation (ChIP) was carried out in HEY cells, and the results showed that FOXM1 could bind to the WBP11 promoter directly (Fig. 4G). To investigate whether WBP11 is involved in the FOXM1-mediated malignant behaviors of OC cells, FOXM1-overexpressing SKOV3 cells were transiently transfected with WBP11-targeted siRNA. As shown in Fig. 4H–J, knockdown of WBP11 successfully impaired cell proliferation, colony formation, migration and invasion induced by FOXM1

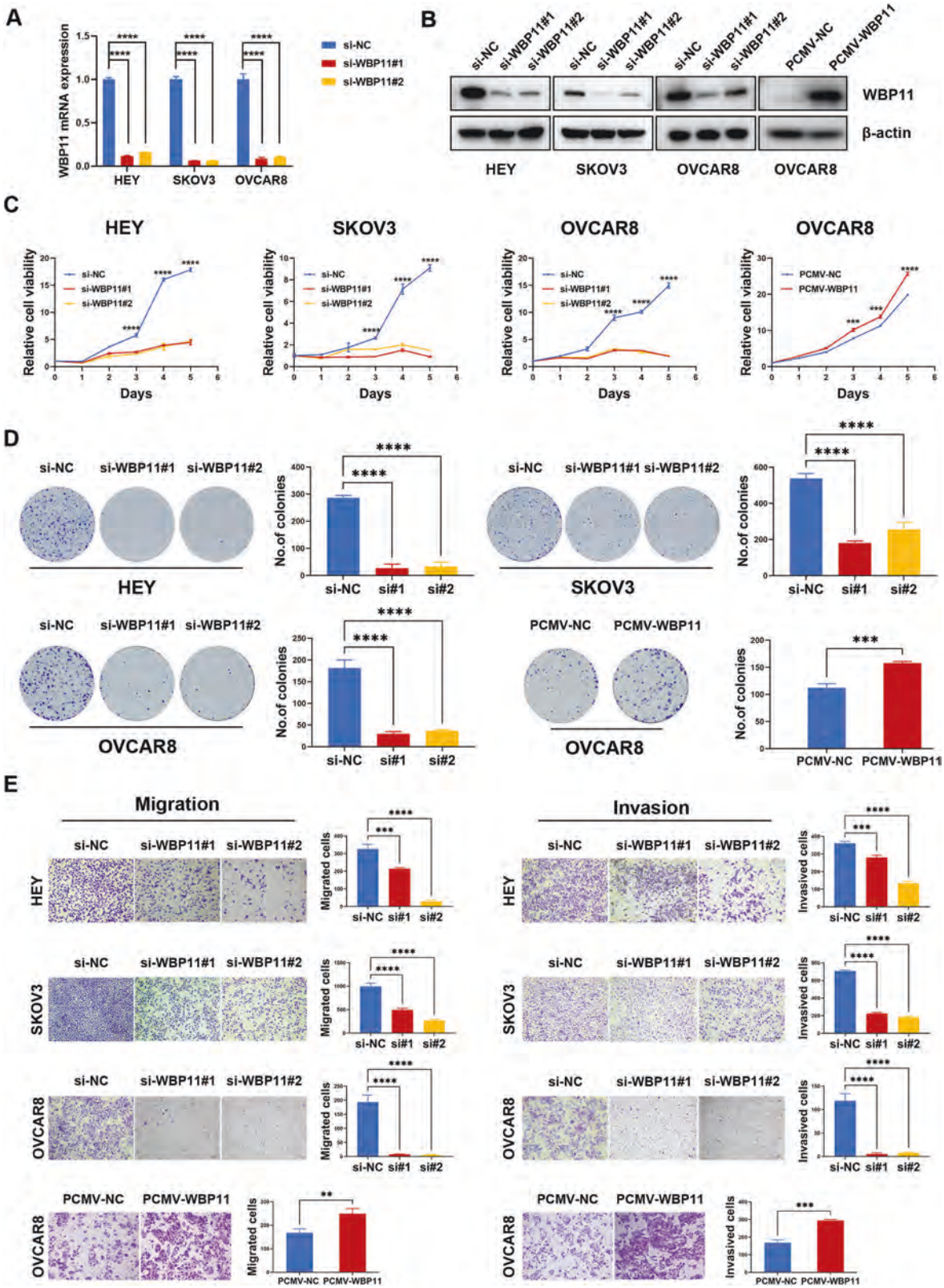

Fig. 2 WBP11 promotes proliferation, migration and invasion of ovarian cancer cells. A WBP11 knockdown efficiency was confirmed by qRT-PCR ($n = 3$ biologically independent samples). **B** WBP11 knockdown and overexpression efficiency was confirmed by western blotting ($n = 3$ biologically independent samples). **C** Growth curve showed the growth of ovarian cancer cells upon WBP11 knockdown or overexpression ($n = 3$ biologically independent samples). **D** Clonogenic assays upon WBP11 knockdown and overexpression in ovarian cancer cells ($n = 3$ biologically independent samples). **E** Transwell migration and invasion assays upon WBP11 knockdown and overexpression in ovarian cancer cells ($n = 3$ biologically independent samples). *P*-value was obtained by Unpaired t-test. Results represent the mean ± SD of three independent experiments. $^{**}P < 0.01$, $^{***}P < 0.001$, $^{****}P < 0.0001$.

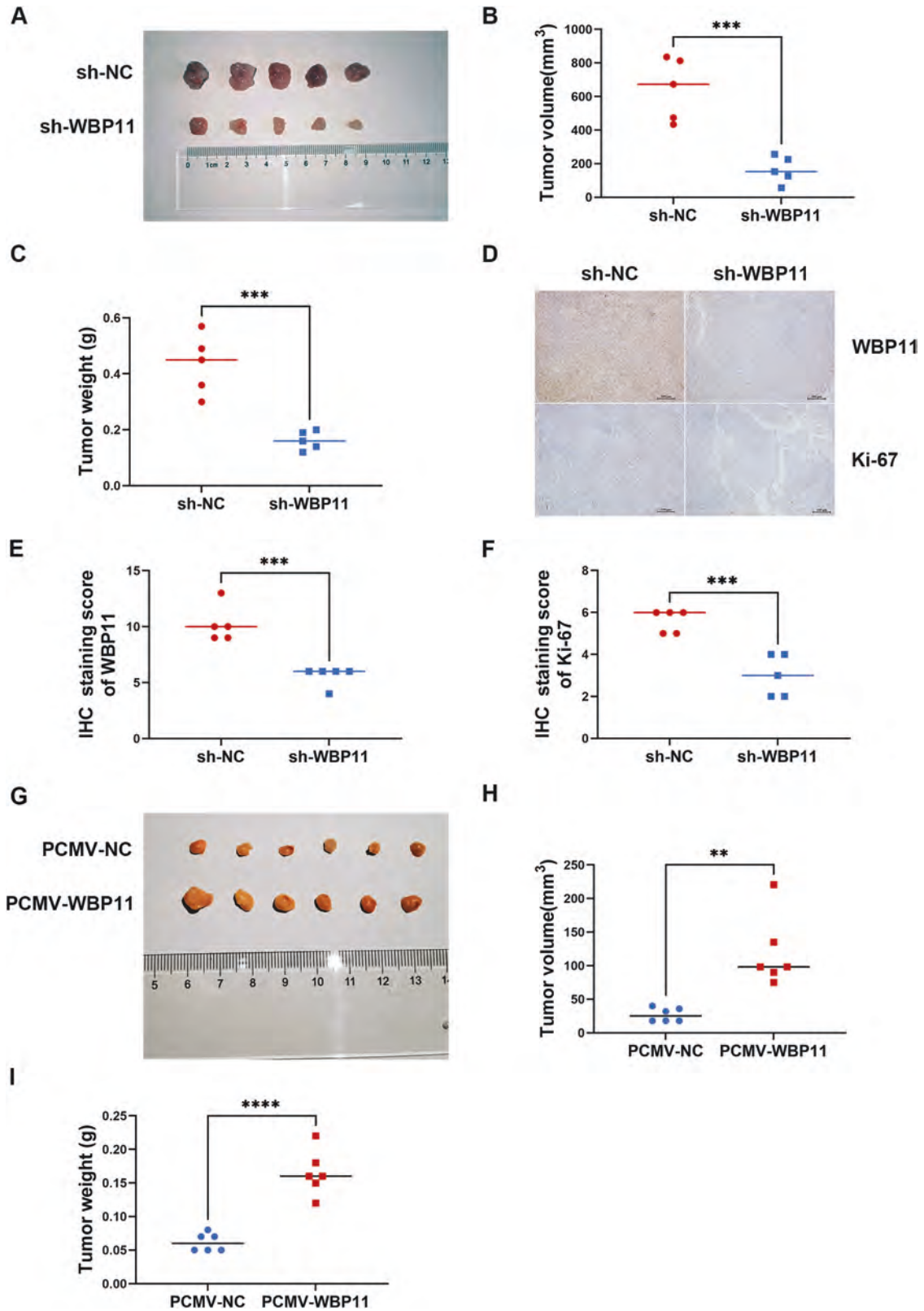

Fig. 3 Knockdown of WBP11 suppresses xenograft tumor growth in vivo. A Images of tumors isolated from subcutaneous injection of nude mice with dox-inducible WBP11 knockdown or control OVCAR8 cells ($n = 5$ per group). **B** Tumor size statistics of WBP11 knockdown or control cells. **C** Tumor weight statistics of WBP11 knockdown or control cells. **D** The WBP11 and Ki-67 expression levels were evaluated by immunohistochemical staining in xenograft tumors from WBP11 knockdown and control cells treated nude mice. **E** IHC staining score statistics of WBP11. **F** IHC staining score statistics of Ki67. **G** Xenograft experiments showed WBP11 overexpression promotes tumor growth in vivo ($n = 6$ mice per group). **H** The size of xenografts tumors with WBP11 overexpression or control cells were compared. **I** The xenografts tumors of WBP11 overexpression or control cells were weighed and compared. *P*-value was obtained by Unpaired t-test. Results represent the mean ± SD. $^{**}P < 0.01$, $^{***}P < 0.001$, $^{****}P < 0.0001$.

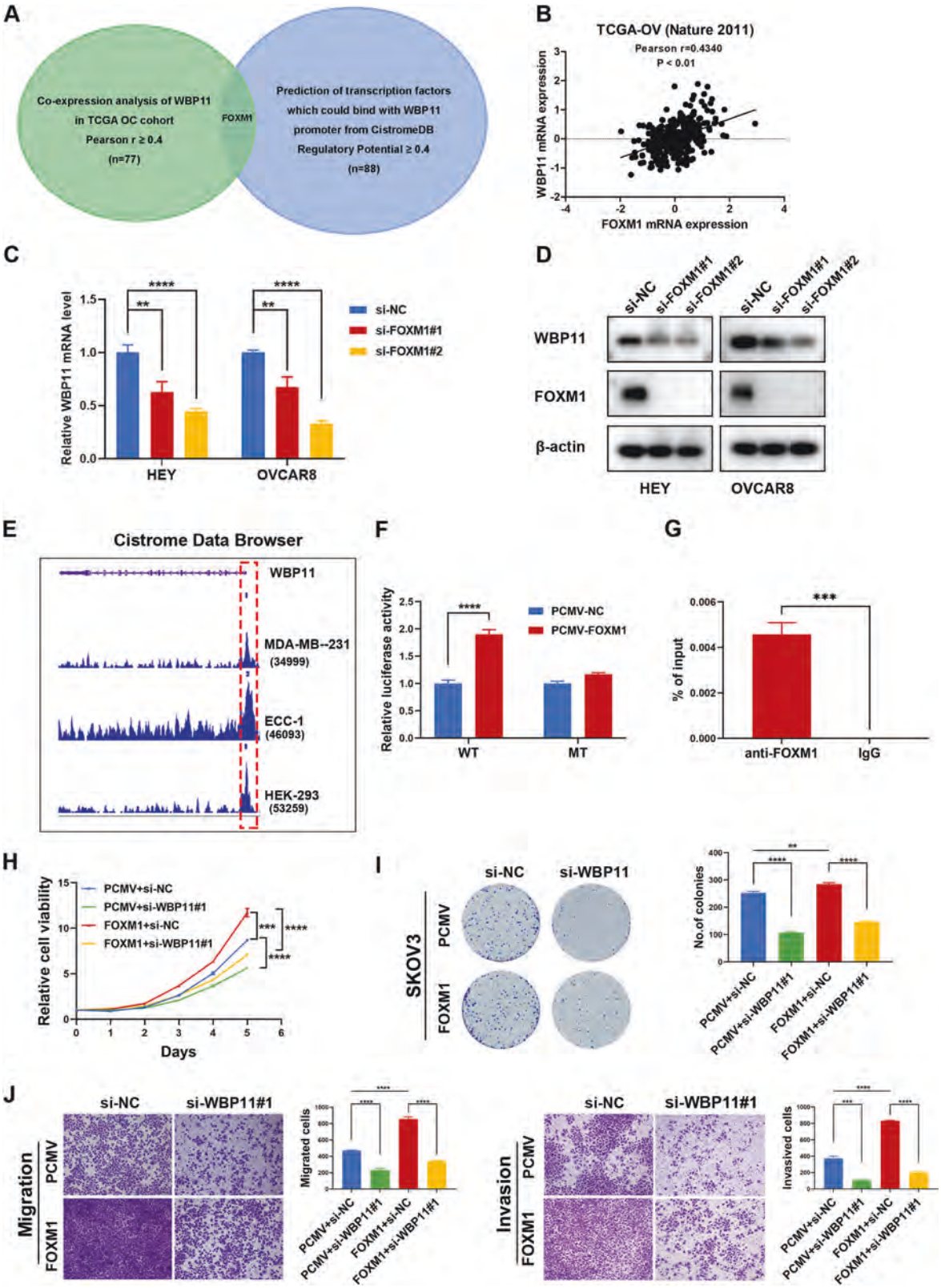

overexpression. Ectopic expression of WBP11 rescued the inhibition of proliferation, migration and invasion induced by silencing FOXM1 in OVCAR8 cells (Supplementary Fig. S1D–F). In Collectively, these data demonstrated that FOXM1 contributes to the high expression of WBP11 in OC cells.

MCM7 is the critical downstream target of WBP11 based on RNA-seq analysis

To determine the regulatory mechanism by which WBP11 promotes malignant behaviors in OC cells, we performed RNA sequencing in WBP11-knockdown and control HEY cells. A

Fig. 4 FOXM1 activates WBP11 transcription in OC cells. A Integrated analysis of transcription factors that could bind to the promoter of WBP11 using CistromeDB (regulatory potential ≥0.4) and coexpresed genes of WBP11 in TCGA OC data from the cBioPortal website (Pearson r ≥ 0.4). **B** Co-expression analysis between WBP11 and FOXM1 expression from TCGA OC cohort. The mRNA and protein levels of WBP11 in ovarian cancer cells with or without FOXM1 knockdown were measured by qRT-PCR (**C**) and western blotting (**D**) ($n = 3$ biologically independent samples). **E** Analysis of FOXM1 binding peaks on WBP11 promoter region in multiple cell lines based on Cistrome Data Brower database. **F** Dual-luciferase reporter assays showing that FOXM1 overexpression increased the luciferase activity of the WT plasmid of WBP11 but not the MT plasmid in HEK293T cells ($n = 3$ biologically independent samples). **G** ChIP-qPCR analysis showed that FOXM1 could bind to the WBP11 promoter region directly in HEY cells ($n = 3$ biologically independent samples). Growth curve assay (**H**) and clonogenic assays (**I**) showed WBP11 knockdown successfully reversed the effect of FOXM1 overexpression on the growth of ovarian cancer cells ($n = 3$ biologically independent samples). **J** Transwell assay showed WBP11 knockdown successfully reversed the effect of FOXM1 overexpression on the migration and invasion capacity in SKOV3 cells ($n = 3$ biologically independent samples). *P*-value was obtained by Unpaired t-test. Results represent the mean ± SD. $^{**}P < 0.01$. $^{***}P < 0.001$, $^{****}P < 0.0001$.

heatmap display of the differentially expressed genes (DEGs) is presented in Fig. 5A (|log2FC| ≥ 0.58 and padj < 0.05). The results of Gene Ontology analysis showed that DEGs were enriched in the regulation of transcription, cell differentiation, cell adhesion, regulation of gene expression, and cell proliferation (Fig. 5B). We performed alternative splicing (AS) analysis, and 1528 genes related to differential AS events were identified after WBP11 knockdown (|IncLevelDifference| > 0.1, FDR < 0.05). Differential AS events including retained introns (RI), skipped exons (SE), alternative 5′ splice sites(A5SS), alternative 3′ splice sites (A3SS), and mutually exclusive exons (MXE), among which SE and RI account for the highest proportion (Fig. 5C). To identify the critical DEGs involved in the process of alternative splicing, we performed integrated analysis of genes downregulated after WBP11 knockdown, 1528 genes involved in the differential alternative splicing events after WBP11 knockdown, and differentially expressed proteins between OC and normal ovary tissues from CPTAC ($p < 0.01$) (Fig. 5D); 14 critical DEGs were identified (Fig. 5E). The relative expression of 14 DEGs in OC tissues and ovary tissues was analyzed, and the results showed that 5 DEGs were overexpressed in OC samples (Fig. 5F). Furthermore, correlation analysis was performed between WBP11 and 5 DEGs in the TCGA-GTEx cohort (Fig. 5G). In order to identify the critical alternative splicing events, we focused on the RI. Integrated analysis of genes downregulated after WBP11 knockdown, 374 genes involving in the intron retention after WBP11 knockdown, and differentially expressed proteins between OC and normal ovary tissues from CPTAC ($p < 0.01$) was performed, only MCM7 and PLCD1 were identified (Fig. 5H). MCM7 (minichromosome maintenance complex component 7) is critical for licensing DNA replication and is involved in the formation and progression of a variety of tumors. Repression of origin licensing is emerging as a promising strategy for suppressing cell proliferation. In response to WBP11 inhibition, increased intron retention of MCM7 was observed (Fig. 5I). Therefore, we selected MCM7 for further study. To provide further evidence of the regulatory role of WBP11 on MCM7, we examined the mRNA and protein levels of MCM7 after WBP11 knockdown. Both the mRNA levels and the protein levels decreased markedly (Fig. 5J–K, Supplementary Fig. S2D), overexpression of WBP11 had an opposite effect (Supplementary Fig. S1G, H). Taken together, these results indicate that MCM7 functions as a critical downstream target of WBP11 in OC cells.

WBP11 facilitates the efficient splicing of MCM7 intron 4

To investigate the regulatory mechanism by which WBP11 regulates MCM7 expression in OC cells, the splice variants of MCM7 mRNA were analyzed through the Ensembl genome browser. Intron 4 was retained in the MCM7–210 transcript (unspliced intron 4) by comparison with the protein-coding transcript variant MCM7–201 (spliced intron 4) (Fig. 6A). Retained intron 4 of MCM7 could induce a stop codon (TAA) in an open reading frame, resulting in premature termination of translation, and could not produce normal MCM7 protein. Then, we examined the relative expression of MCM7–201 and MCM7–210 transcripts in OC and normal control tissues in the TCGA and GTEx databases, and the MCM7–201 transcript was found to be significantly upregulated in OC tissues compared with normal ovary tissues, but there was no significant difference between OC tissues and FT tissues, probably because of the limited number of FT samples. There was no expression difference in the MCM7–210 transcript in OC samples, normal ovary samples and FT samples (Fig. 6B). WBP11 expression was positively associated with MCM7-201 expression in OC tissues according to correlation analysis (Fig. 6C). Specific primers were designed to span intron 4 within exons 4 and 5, and qRT–qPCR was applied to detect MCM7 transcript expression after WBP11 knockdown in OC cells. Consistently, we found an increase in the level of the unspliced transcript variant of MCM7 (MCM7–210), and the level of the spliced transcript variant of MCM7 (MCM7–201) was markedly reduced (Fig. 6D, E). As expected, the spliced transcript variant of MCM7 (MCM7–201) was increased after WBP11 overexpression (Supplementary Fig. S1I). The proportion of unspliced MCM7 transcripts was increased after WBP11 knockdown (Fig. 6F), whereas WBP11 overexpression had the opposite effect (Supplementary Fig. S1J). Moreover, we assessed the effect of WBP11 expression on the RNA decay rate through an RNA stability assay in SKOV3 cells, and the half-life of MCM7 mRNA was found to be prolonged after WBP11 overexpression (Fig. 6G). To further demonstrate that the WBP11 protein could bind to downstream MCM7 pre-mRNA, we performed RNA immunoprecipitation PCR, and the results showed that MCM7 mRNA was significantly enriched in WBP11 overexpression precipitates compared with the IgG control precipitate (Fig. 6H). PQBP1 and TUBGCP6 RNA levels were also examined in WBP11-overexpressing precipitates and in IgG control (Fig. 6H). In summary, WBP11 promotes MCM7 alternative splicing by repressing intron retention.

MCM7 knockdown decreased the malignant phenotype of WBP11 overexpression

Next, we studied the biological function of MCM7 in OC cells. MCM7-targeted siRNA and si-NC were transiently transfected into OC cells. MCM7-overexpressing plasmid and control plasmid was transiently transfected into SKOV3 cells. Knockdown and overexpression efficiency was verified by qRT–PCR and western blotting (Fig. 7A, B, Supplementary Fig. S2E, S3A). The CCK-8 proliferation assay showed that MCM7 silencing obviously decreased the growth rate of HEY and OVCAR8 cells and MCM7 overexpression had the opposite effect in SKOV3 cells (Fig. 7C). In addition, colony formation ability was suppressed after MCM7 knockdown, and enhanced following MCM7 overexpression (Fig. 7D, Supplementary Fig. S3B). Transwell assays demonstrated that the cell migratory and invasive abilities significantly decreased after MCM7 silencing (Fig. 7E). These results indicated that MCM7 mediates the proliferation and metastasis of OC cells. To explore whether MCM7 contributes to the WBP11-mediated malignant behaviors of OC cells, we performed rescue experiments by transiently transfecting MCM7-targeted siRNA into WBP11-overexpressing OVCAR8 cells. As expected, MCM7 inhibition in WBP11-overexpressing cells significantly affected cell proliferation, migration and invasion (Fig. 7F, G). Moreover, overexpression of MCM7 in HEY cells rescued the

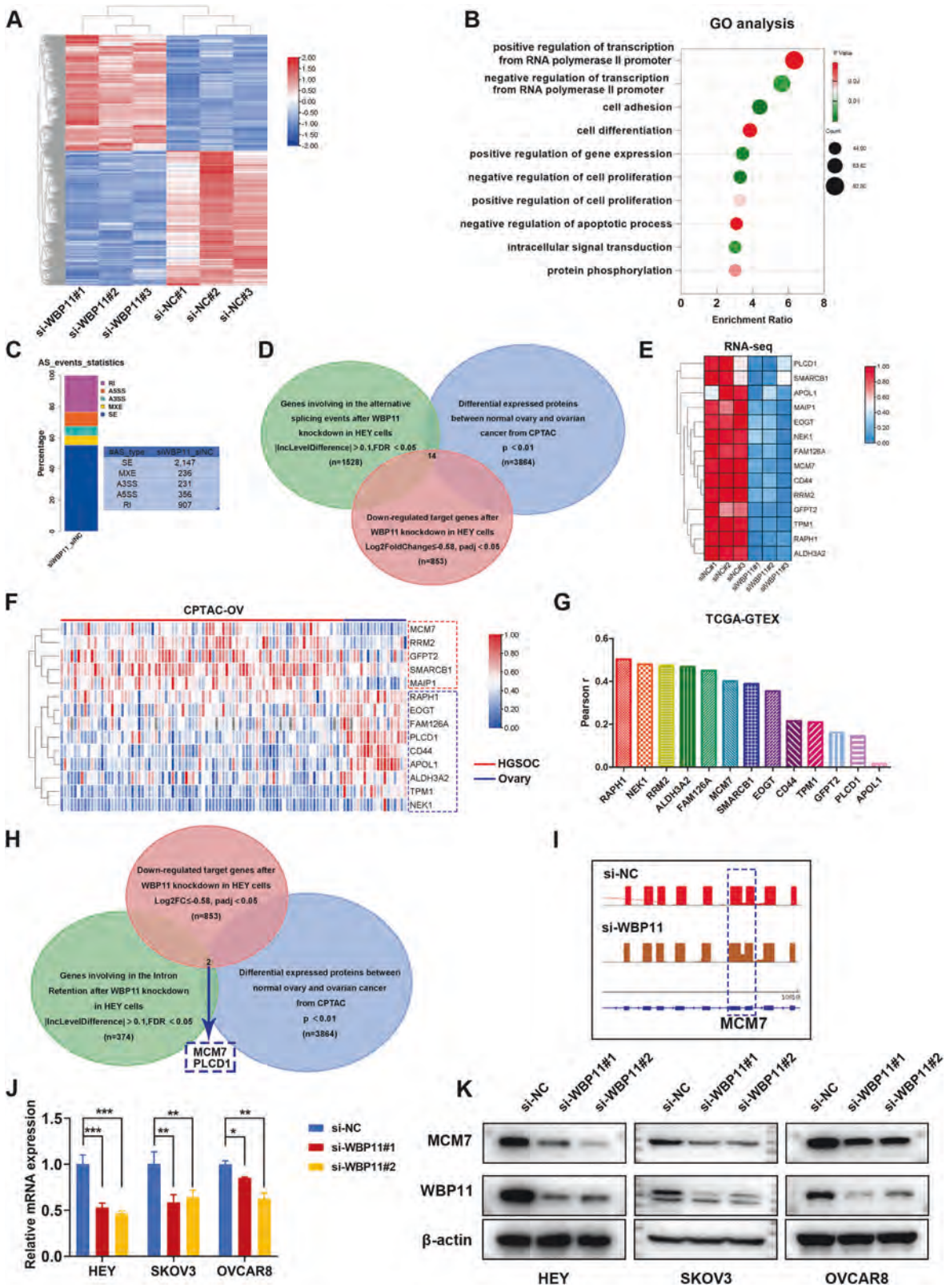

inhibition of proliferation, migration and invasion induced by silencing WBP11 (Fig. 7H, Supplementary Fig. S3C). These results demonstrate that WBP11 promotes the malignant progression of OC cells by regulating MCM7 expression and that MCM7 is the key downstream target of WBP11 in OC cells.

ASO-mediated WBP11 knockdown suppresses the proliferation and mobility of OC cells

Recently, antisense oligonucleotide (ASO) drugs have attracted interest owing to their ability to target diverse RNAs. To explore whether WBP11 could be blocked by ASOs, we designed three

Fig. 5 MCM7 functions as a downstream target of WBP11 based on RNA-seq analysis. A Heatmap of differential expression genes from RNA-seq analysis of WBP11 knockdown and control in HEY cells. **B** Bubble chart showing the results of Gene Ontology (GO) analysis of differential expression genes described in **A**. **C** Chart depicting the proportions of different types of AS events in the RNA-seq data from HEY cells after WBP11 knockdown. SE skipped exons, RI retained introns, A5SS alternative 5′ splice site, A3SS alternative 3′ splice site, MXE mutually exclusive exons. **D** Venn diagram showing 1528 genes involving in alternative splicing events after WBP11 knockdown and differentially expressed proteins between normal ovary and ovarian cancer of CPTAC database and down-regulated target genes after WBP11 knockdown in HEY cells. **E** Heatmap of differential expression of selected genes ($n = 14$) described in **D**. **F** The differential expression of selected genes in HGSOC ($n = 84$) compared to normal ovaries ($n = 19$) from CPTAC database. **G** Schematic diagram showing correlation analysis between WBP11 and genes described in **F**. **H** Venn diagram showing 853 genes downregulated after WBP11 knockdown, 374 genes involving in the intron retention after WBP11 knockdown, and differentially expressed proteins between OC and normal ovary tissues from CPTAC. **I** Schematic diagram of RNA-seq reads mapping to MCM7 in HEY cells in response to WBP11 knockdown. **J** qRT-PCR analysis of MCM7 mRNA expression after WBP11 inhibition in ovarian cancer cells ($n = 3$ biologically independent samples). **K** Western blotting showed the WBP11 and MCM7 protein levels after WBP11 downregulation. *P*-value was obtained by Unpaired t-test. $^{*}P < 0.05$, $^{**}P < 0.01$, $^{***}P < 0.001$.

ASOs specifically targeting WBP11 for further study. HEY and SKOV3 cells were transfected with three independent ASOs. WBP11 expression was significantly inhibited by the three ASOs in HEY and SKOV3 cells (Fig. 8A). Accordingly, MCM7 expression was decreased when WBP11 was suppressed (Fig. 8B). CCK-8 and Transwell assays showed that the proliferation, migration, and invasion abilities were decreased after the use of WBP11 ASO2 (Fig. 8C–E). Moreover, we established a PDX tumor model to assess the therapeutic effects of ASOs in OC patients. When subcutaneous tumors reached 5 mm in diameter, we divided the PDX tumor model mice into the NC group ($n = 4$) and ASO group ($n = 4$). Compared to the NC group, the weight and volume of tumors in the ASO treatment group were significantly lower (Fig. 8F–H). These results suggested that ASO-mediated WBP11 knockdown suppresses the proliferation and mobility of OC cells.

DISCUSSION

Pre-mRNA splicing is essential in eukaryotic gene expression and is an important regulatory mechanism [4, 15]. Increasing evidence has shown that dysregulated expression of splicing factors and aberrant splicing can drive oncogenesis [16, 17]. WBP11 is recognized as a pre-mRNA splicing factor and is required for centriole duplication through splicing the TUBGCP6 pre-mRNA [13]. However, it is unclear how WBP11 exerts its splicing function in OC. In this study, we found that WBP11 was commonly overexpressed in OC and that high expression of WBP11 was correlated with a poor prognosis in OC patients. We next investigated the biological function of WBP11 and found that WBP11 promoted the malignant biological behavior of OC cells in vitro and in vivo. This is consistent with previous reports on gastric cancer [14]. Herein, for the first time, we demonstrated that WBP11 is an oncogene in OC and could be a vital prognostic biomarker of OC.

Moreover, we investigated the potential transcription factors involved in the regulation of WBP11. FOXM1 is involved in cell proliferation, self-renewal and tumorigenesis [18]. FOXM1 has been identified in humans as a proto-oncogene that facilitates most of the hallmarks of malignancy [19, 20]. Increased FOXM1 expression in multiple cancers, including hepatocellular carcinoma [21], small cell lung cancer [22], has been reported. FOXM1 is activated in 87% of OC samples in the TCGA [23], and high FOXM1 expression predicts a poor prognosis and promotes proliferation, migration and invasion in OC cells [24]. In our study, FOXM1 knockdown led to a decrease in WBP11 expression. Moreover, WBP11 inhibition successfully impaired the effect of FOXM1 overexpression on the malignant behaviors of OC cells. FOXM1 could bind with the WBP11 promoter directly and transactivate WBP11 transcription in OC cells. These results indicated that WBP11 is a direct transcriptional target of FOXM1. Next, to identify alternative splicing (AS) events, RNA-seq was performed. rMATS analysis and RT–PCR validation determined that intron 4 of MCM7 was retained upon WBP11 knockdown in OC cells. RNA immunoprecipitation (RIP) assay demonstrating that WBP11 can bind MCM7 RNA. We also examined PQBP1 and TUBGCP6 RNA levels, and the results showed that PQBP1 and TUBGCP6 levels were significantly higher in WBP11-overexpressing precipitates than in IgG controls, consistent with reports in the literature [11, 13]. In addition, WBP11 increased the stability of MCM7 mRNA.

The minichromosome maintenance complex (MCM) is required for licensing replication origins and advancing replication, and reduced expression of MCM protein leads to genomic instability [25]. MCM7 has been suggested to promote cell proliferation in hepatocellular carcinoma and promotes stemness in bladder cancer [26, 27]. In this study, we confirmed that MCM7 knockdown suppressed the malignant behaviors of OC cells and restored the effect of WBP11 overexpression on the proliferation and metastasis of OC cells.

Oligonucleotides—including antisense oligonucleotides (ASOs)—have emerged as a third class of therapeutic modalities [28]. The ASO nusinersen is the first antisense drug to become a notable commercial success [29]. Although all approved ASOs are for rare diseases, preclinical work suggests that antisense oligonucleotides might also have therapeutic value in oncology. A BUD31-targeted ASO mediates BCL2L12 exon 3 skipping to induce cell apoptosis and suppress cell proliferation in OC xenografts [30]. A number of clinical trials on ASOs are ongoing. Here, we designed ASOs to target WBP11, which resulted in MCM7 inhibition. ASOs suppressed the proliferation and metastasis of OC cells in vitro and inhibited the growth of OC xenografts in a PDX model. ASOs targeting WBP11 are a promising strategy for OC.

MATERIALS AND METHODS

Patients and tissue samples

Fifteen fresh-frozen OC samples and 19 fallopian tube tissues, 4 normal ovary tissues were used to perform qRT–PCR and western blotting. A total of 194 OC and 74 normal fallopian tube samples were used for the tissue microarray (TMA). All the samples were from patients at Qilu Hospital of Shandong University from 2005 to 2022, and all the participants provided informed consent. Ethical approval was obtained from the Ethics Committee of Qilu Hospital, Shandong University (KYLL-202209-032).

Bioinformatics analysis

Differentially expressed genes between normal ovary and OC samples were obtained from the GEPIA2.0 database (http://gepia.cancer-pku.cn/). The differentially expressed protein data were from the Clinical Proteomic Tumor Analysis Consortium (CPTAC) (https://cptac-data-portal.georgetown.edu/studies). The clinical prognostic value of WBP11 in ovarian cancer was evaluated on the Kaplan–Meier Plotter website (http://kmplot.com/).

Cell lines and cell culture

HEY cells were from the laboratory of Jian-Jun Wei. OVCAR8 cells were a kind gift from Dr. Ma's laboratory. SKOV3 and HEK293T cell lines were purchased from the Shanghai Cell Library of the Chinese Academy of Sciences. HEY and HEK293T cells were maintained in DMEM (Gibco).

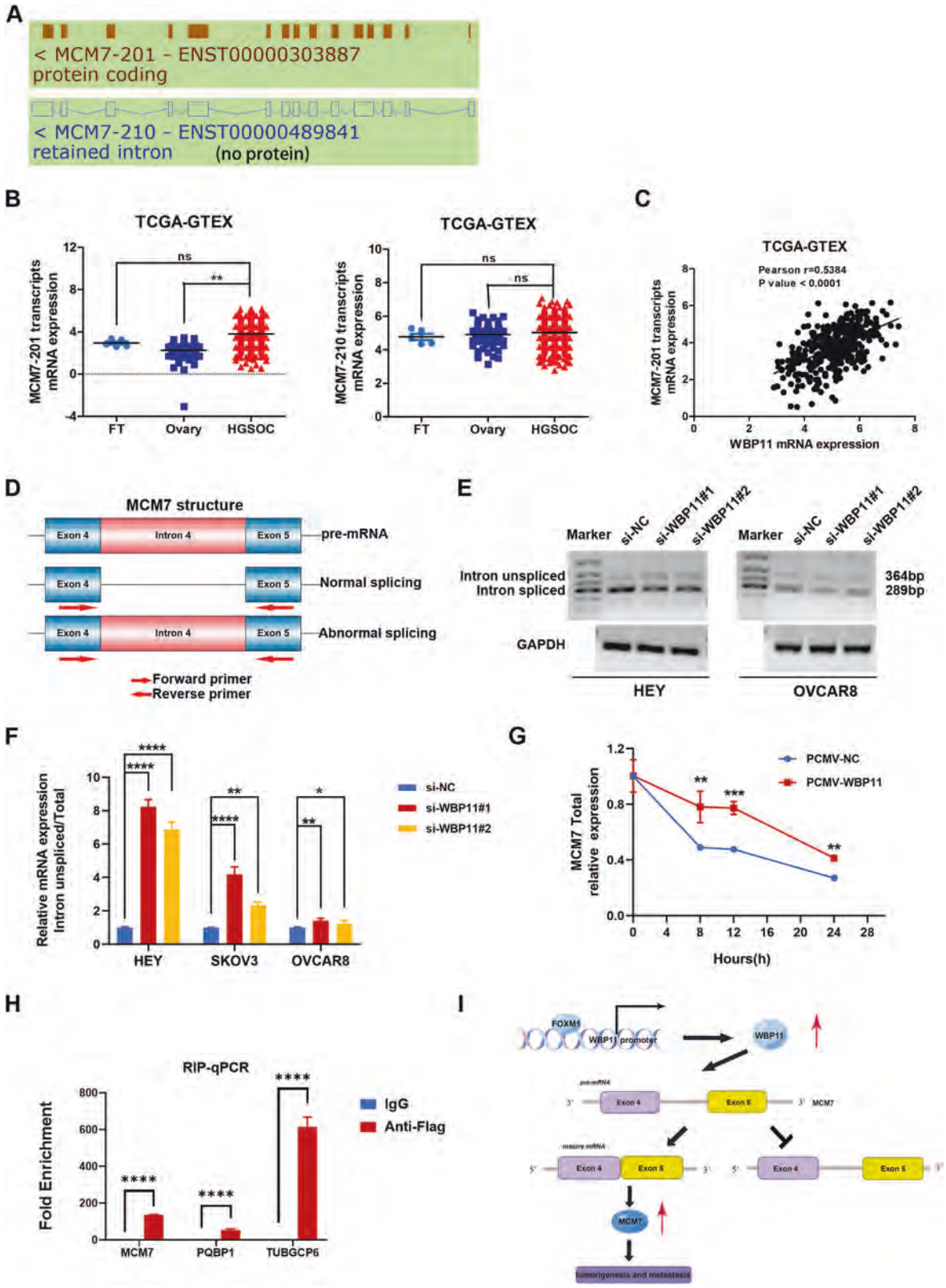

OVCAR8 cells were maintained in RPMI 1640 (Gibco), and SKOV3 cells were cultured in McCoy's 5 A medium. All the medium types were supplemented with 10% fetal bovine serum (FBS) and cultured in a humidified incubator at 37 °C in 5% CO2. The identities of all the cell lines were authenticated by short tandem repeat (STR) profiling.

Lentiviral infection and RNA interference

The open reading frames (ORFs) of WBP11 were synthesized by Vigene Bioscience (Jinan, China). OC cells were transfected with lentivirus and selected with puromycin at 2 μg/ml to obtain stable cell lines. Small interfering RNAs (siRNAs) targeting WBP11, MCM7, and FOXM1 were

Fig. 6 WBP11 facilitates efficient splicing of MCM7 intron. A Schematic diagram showing two splicing variants of the MCM7 mRNA transcript identified from the Ensemble genome browser. **B** Relative mRNA expression of MCM7 splicing variants described in **A** from TCGA ovarian cancer database ($n = 426$). **C** Correlation analysis between MCM7-201 variants and WBP11 mRNA in ovarian cancer tissues from TCGA ovarian cancer ($n = 426$). **D** Schematic illustration showing the position of intron retention and primers used for RT-PCR. **E**, **F** Agarose gel electrophoresis and RT-PCR was used to analyze the splicing isoforms of MCM7 in ovarian cancer cells with WBP11 inhibition ($n = 3$ biologically independent samples). **G** The decay rate of mRNA of MCM7 at the indicated times after actinomycin D (5 μg/ml) treatment in SKOV3 PCMV-NC cells and PCMV-WBP11 cells ($n = 3$ biologically independent samples). **H** RIP-qPCR validation of interaction between WBP11 and MCM7 mRNA in HEY cells overexpressing FLAG-WBP11. FLAG antibody was used for immunoprecipitation. PQBP1 and TUBGCP6 served as a positive control ($n = 3$ biologically independent samples). **I** Schematic illustration showing that WBP11 is transcriptionally activated by FOXM1. WBP11 promotes ovarian cancer progression by regulating efficient splicing of MCM7 intron. This figure was drawn by Figdraw. *P*-value was obtained by Unpaired t-test. $^{*}P < 0.05$, $^{**}P < 0.01$, $^{***}P < 0.001$, $^{****}P < 0.0001$.

synthesized by GenePharma (Shanghai, China). Plasmids of MCM7 overexpression or control were synthesized by Vigene Bioscience (Jinan, China). Plasmids and siRNA were transfected using Lipofectamine 2000 (Invitrogen, USA). RNA was extracted 24 h after transfection, and protein was extracted 48–72 h after transfection.

RNA isolation and qRT–PCR

RNA from tissue was extracted by TRIzol reagent (Invitrogen, USA), and RNA from cells was isolated with the RNA extraction kit (FORE GENE). RNA was transcribed into cDNA using PrimeScript RT Master Mix kits (Takara, RR037A). qRT–PCR was performed using SYBR Green qPCR Master Mix (Takara, RR420A). The primer sequences are listed in Supplementary Table S1.

Protein extraction and western blotting

Tissues or cells were lysed on ice with RIPA lysis buffer (Beyotime, China), followed by sonication. The lysate was centrifuged, and the supernatant was collected. The protein was separated with SDS–PAGE, and gels were transferred onto PVDF membranes (Merck Millipore, USA). After blocking with 5% skimmed milk for 1 h, the membranes were incubated with the indicated primary antibodies at 4 °C overnight. The membranes were washed and incubated with secondary antibodies for 1 h on the following day. Finally, the bands were detected with ECL reagents (GE Health care). β-Actin was used as the endogenous control. The primary antibodies for western blotting are listed below: anti-FOXM1(1:1000, CST, #20459), anti-WBP11 (1:2000, Abcam, ab154590), anti-MCM7 (1:1000, CST, #3735), and anti-β-actin (1:8000, Sigma–Aldrich, SAB3500350).

Cell proliferation assay

Cells were plated in 96-well plates at 1000 cells/well and incubated with 10 μl CCK-8 solution per well for 4 h. The absorbance at 450 nm was quantified by a microplate spectrophotometer.

Clonogenic assays

Cells (800–1000) were cultured at 37 °C for 8–14 days. The colonies were further methanol-fixed and stained with crystal violet. Finally, the colony formation ability was evaluated based on the number of colonies formed.

Cell migration and Matrigel invasion assay

For invasion assays, the surface of the Transwell membrane was coated with a layer of Matrigel. Cells in serum-free medium were seeded in the upper chamber, whereas the lower chamber was filled with 20% fetal bovine serum. After incubation in a 37 °C incubator, the chamber was fixed and stained. The migrated or invaded cells were observed under a light microscope.

Immunohistochemistry (IHC)

Immunohistochemical staining was conducted with a two-step immunohistochemistry method (Zhongshan Goldenbridge, Beijing, China) according to the protocol. Tissue sections were cut into 4-μm-thick slices, deparaffinized and dehydrated. Next, antigen retrieval was conducted with citrate acid repair buffer (pH 6.0) or EDTA buffer (pH 9.0). After endogenous peroxidase was blocked, slides were incubated with primary antibodies at 4 °C overnight. On the next day, the slides were incubated with secondary antibodies, and DAB was used for visualization. The results of immunohistochemical staining were evaluated according to area and intensity. The antibodies used in the IHC assay were as follows: anti-WBP11 (1:500, Abcam, ab154590) and anti-Ki-67 (1:200, CST, 9449T).

RNA sequencing analysis

WBP11-targeted siRNA was transfected into HEY cells, and total RNA was extracted using TRIzol reagent. Next-generation sequencing was performed by Annoroad Genomics Co., Ltd, China. The threshold for differentially expressed genes was $|\text{FoldChange}| \geq 0.58$ and $p < 0.05$.

RNA immunoprecipitation (RIP) assay

WBP11 with a FLAG tag was ectopically expressed in HEY cells. RIP assays were performed with an RNA-Binding Protein Immunoprecipitation Kit (Millipore, 17–700) according to the manufacturer's instructions. An anti-FLAG antibody was used for immunoprecipitation, and IgG was used as a control. Finally, qRT–PCR was performed to assess the enrichment of MCM7 mRNA in the anti-FLAG antibody group compared to the IgG control group.

Luciferase assay

A luciferase assay was conducted with a dual-luciferase reporter kit from Promega (E2920) in HEK293T cells. The wild-type and mutant promoters of WBP11 were cloned into PGL4.26 plasmids separately. Luciferase activity was measured 48 h after transfection, and the relative firefly/Renilla activity was calculated to evaluate the effect of the transcriptional activity of FOXM1 on the WBP11 promoter.

Chromatin immunoprecipitation assay

The chromatin immunoprecipitation (ChIP) assay was performed using a ChIP assay kit (Millipore). Anti-FOXM1 (CST, #20459) or IgG rabbit antibodies were used for immunoprecipitation. The purified DNA was analyzed by q-PCR.

Tumor xenograft models

Female BALB/c nude mice (5-week-old) were purchased from Gem Pharma tech (Nanjing, China) and were randomly divided into two groups (5–6 mice per group). Mice were housed in a specific pathogen-free (SPF) environment and all the mice were injected subcutaneously with doxycycline-induced WBP11 knockdown OVCAR8 cells or WBP11 overexpression OVCAR8 cells. In the experimental group, mice injected with doxycycline-induced WBP11 knockdown OVCAR8 cells were fed with doxycycline (1.2 g/L) mixed with 5% sucrose, while in the control group, mice were fed with 5% sucrose alone. The mice were sacrificed, and the tumors were isolated, and the tumor weight and volume were measured. The expression of WBP11 and Ki-67 in xenograft tumors was determined by IHC. The animal experiment was approved by the Animal Care and Use Committee of Qilu Hospital, Shandong University (Dwll-2022-050).

PDX model

Fresh primary ovarian cancer tissues were extracted at Qilu Hospital. The tissues were cut into pieces and implanted subcutaneously into NCG (NOD-Prkdc^{em26Cd52}Il2rg^{em26Cd22}/Gpt) mice (Gem Pharmatech) labeled passage 0 (P0). When the tumor size reached 1 cm^3, the tumor was harvested and subcutaneously injected into passage 1 (P1) NCG mice. When the tumors of P1 mice reached 1 cm^3, the tumors were implanted into passage 2 (P2) mice. We established eight P2 mice simultaneously, and the mice were randomly assigned to the ASO group and NC group. ASO (Genepharma) or NC (Genepharma) was injected intratumorally when

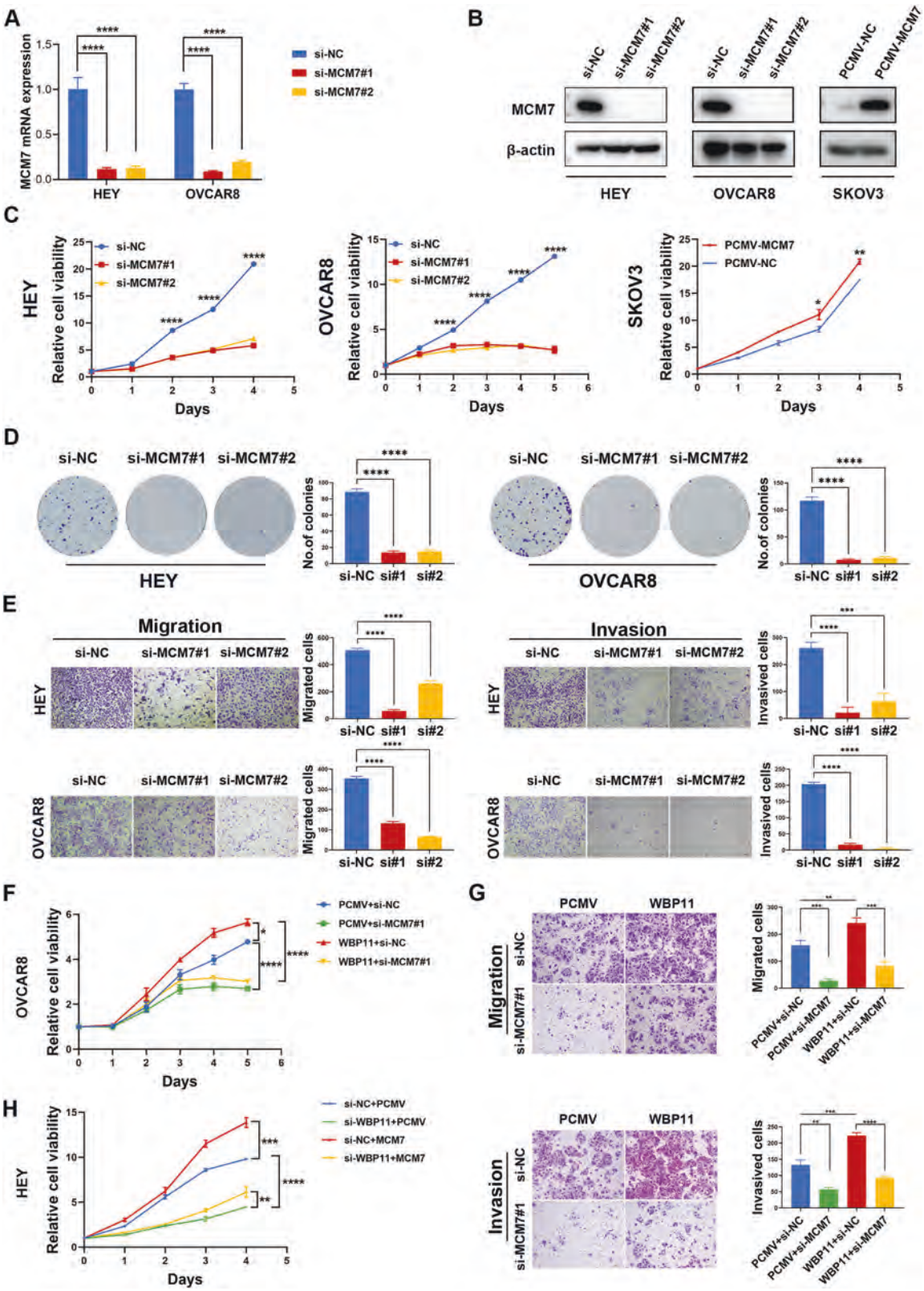

Fig. 7 Knockdown of MCM7 impaired the phenotype of WBP11 overexpression. A MCM7 knockdown efficiency was confirmed by qRT-PCR ($n = 3$ biologically independent samples). **B** MCM7 knockdown and overexpression efficiency was confirmed by western blotting. **C** Growth curve and **D** clonogenic assay were used to evaluate the effect of MCM7 on the proliferation of ovarian cancer cells ($n = 3$ biologically independent samples). **E** Migration and invasion capacity of HEY, OVCAR8 cells upon MCM7 downregulation ($n = 3$ biologically independent samples). **F** MCM7 knockdown reduced the growth curve of WBP11-overexpressing OVCAR8 cells ($n = 3$ biologically independent samples). **G** MCM7 downregulation partially reversed the effect of WBP11 overexpression on cell migration and invasion ability ($n = 3$ biologically independent samples). **H** MCM7 overexpression partially restored the growth retardation caused by WBP11 inhibition in HEY cells ($n = 3$ biologically independent samples). *P*-value was obtained by Unpaired t-test. $^{**}P < 0.01$, $^{***}P < 0.001$, $^{****}P < 0.0001$.

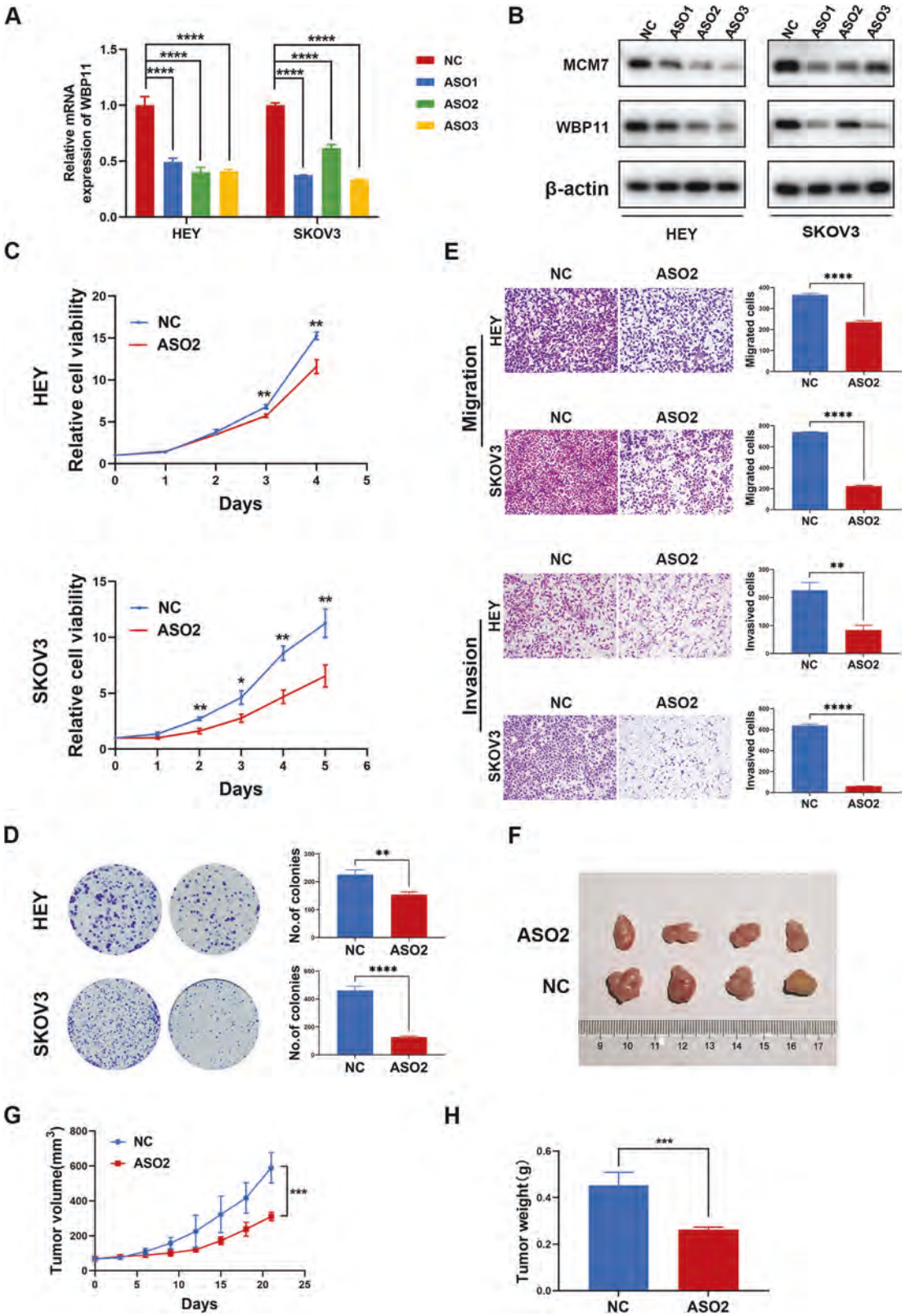

Fig. 8 ASO-mediated MCM7 knockdown suppresses the proliferation and mobility of OC cells. A WBP11 was knockdown by WBP11-targeted ASOs confirmed by q-PCR ($n = 3$ biologically independent samples). **B** WBP11 and MCM7 was knockdown by WBP11-targeted ASOs confirmed by western blotting. **C** CCK-8 assay was performed in ovarian cancer cell lines treated with ASO2 ($n = 3$ biologically independent samples). **D** Colony formation of ovarian cancer cell lines treated with ASO2 ($n = 3$ biologically independent samples). **E** Transwell migration and invasion assays upon ASO2 treatment in ovarian cancer cells ($n = 3$ biologically independent samples). **F** ASO2 intratumoral injection to PDX tumor model. The PDX tumor of ASO group were smaller compared to NC group ($n = 4$ per group). **G** The tumor volume and weight (**H**) were measured for each group. *P*-value was obtained by Unpaired t-test. $^{*}P < 0.05$, $^{**}P < 0.01$, $^{***}P < 0.001$, $^{****}P < 0.0001$.

the established subcutaneous tumor reached 5 mm in diameter. Mice received 5 nmol ASO dissolved in 100 µl sterile PBS every 3 days. All mice were housed in a specific pathogen-free (SPF) environment. Finally, all the mice were anesthetized and sacrificed, and the tumor volume and weight were measured. The animal experiment was approved by the Animal Care and Use Committee of Qilu Hospital, Shandong University (Dwll-2022-050). The sequences of ASO compounds are listed in Supplementary Table S2.

Statistical analysis

Statistical analysis was performed using GraphPad Prism 9. Student's *t* test was chosen to analyze the difference in quantitative data. The log-rank test was used to analyze the clinical prognosis data. The results represent the mean ± SD of three independent experiments. Differences with $P < 0.05$ ($^{*}P < 0.05$, $^{**}P < 0.01$, $^{***}P < 0.001$, $^{****}P < 0.0001$) were considered statistically significant.

DATA AVAILABILITY

The datasets used and/or analyzed during the current study are available from the corresponding author on reasonable request.

REFERENCES

1. Siegel RL, Miller KD, Fuchs HE, Jemal A. Cancer statistics, 2022. CA Cancer J Clin. 2022;72:7–33.
2. Lheureux S, Gourley C, Vergote I, Oza AM. Epithelial ovarian cancer. Lancet. 2019;393:1240–53.
3. Kuroki L, Guntupalli SR. Treatment of epithelial ovarian cancer. BMJ. 2020;371:m3773.
4. Baralle FE, Giudice J. Alternative splicing as a regulator of development and tissue identity. Nat Rev Mol Cell Biol. 2017;18:437–51.
5. Pan Q, Shai O, Lee LJ, Frey BJ, Blencowe BJ. Deep surveying of alternative splicing complexity in the human transcriptome by high-throughput sequencing. Nat Genet. 2008;40:1413–5.
6. Chabot B, Shkreta L. Defective control of pre-messenger RNA splicing in human disease. J Cell Biol. 2016;212:13–27.
7. Craggs G, Finan PM, Lawson D, Wingfield J, Perera T, Gadher S, et al. A nuclear SH3 domain-binding protein that colocalizes with mRNA splicing factors and intermediate filament-containing perinuclear networks. J Biol Chem. 2001;276:30552–60.
8. Galganski L, Urbanek MO, Krzyzosiak WJ. Nuclear speckles: molecular organization, biological function and role in disease. Nucleic Acids Res. 2017;45:10350–68.
9. Agafonov DE, Deckert J, Wolf E, Odenwälder P, Bessonov S, Will CL, et al. Semi-quantitative proteomic analysis of the human spliceosome via a novel two-dimensional gel electrophoresis method. Mol Cell Biol. 2011;31:2667–82.
10. Wahl MC, Will CL, Lührmann R. The spliceosome: design principles of a dynamic RNP machine. Cell. 2009;136:701–18.
11. Iwasaki Y, Thomsen GH. The splicing factor PQBP1 regulates mesodermal and neural development through FGF signaling. Development. 2014;141:3740–51.
12. Martin EMMA, Enriquez A, Sparrow DB, Humphreys DT, McInerney-Leo AM, Leo PJ, et al. Heterozygous loss of WBP11 function causes multiple congenital defects in humans and mice. Hum Mol Genet. 2020;29:3662–78.
13. Park EM, Scott PM, Clutario K, Cassidy KB, Zhan K, Gerber SA, et al. WBP11 is required for splicing the TUBGCP6 pre-mRNA to promote centriole duplication. J Cell Biol. 2020;219:e201904203.
14. Wang L, Yu T, Li W, Li M, Zuo Q, Zou Q, et al. The miR-29c-KIAA1199 axis regulates gastric cancer migration by binding with WBP11 and PTP4A3. Oncogene. 2019;38:3134–50.
15. Gallego-Paez LM, Bordone MC, Leote AC, Saraiva-Agostinho N, Ascensão-Ferreira M, Barbosa-Morais NL. Alternative splicing: the pledge, the turn, and the prestige : The key role of alternative splicing in human biological systems. Hum Genet. 2017;136:1015–42.
16. Rahman MA, Krainer AR, Abdel-Wahab O. SnapShot: Splicing Alterations in Cancer. Cell. 2020;180:208–208.e1.
17. Desterro J, Bak-Gordon P, Carmo-Fonseca M. Targeting mRNA processing as an anticancer strategy. Nat Rev Drug Discov. 2020;19:112–29.
18. Korver W, Roose J, Clevers H. The winged-helix transcription factor Trident is expressed in cycling cells. Nucleic Acids Res. 1997;25:1715–9.
19. Gartel AL. FOXM1 in Cancer: Interactions and Vulnerabilities. Cancer Res. 2017;77:3135–9.
20. Nandi D, Cheema PS, Jaiswal N, Nag A. FoxM1: Repurposing an oncogene as a biomarker. Semin Cancer Biol. 2018;52:74–84.
21. Hu G, Yan Z, Zhang C, Cheng M, Yan Y, Wang Y, et al. FOXM1 promotes hepatocellular carcinoma progression by regulating KIF4A expression. J Exp Clin Cancer Res. 2019;38:188.
22. Liang S-K, Hsu C-C, Song H-L, Huang Y-C, Kuo C-W, Yao X, et al. FOXM1 is required for small cell lung cancer tumorigenesis and associated with poor clinical prognosis. Oncogene. 2021;40:4847–58.
23. Cancer Genome Atlas Research Network. Integrated genomic analyses of ovarian carcinoma. Nature. 2011;474:609–15.
24. Wen N, Wang Y, Wen L, Zhao S-H, Ai Z-H, Wang Y, et al. Overexpression of FOXM1 predicts poor prognosis and promotes cancer cell proliferation, migration and invasion in epithelial ovarian cancer. J Transl Med. 2014;12:134.
25. Machida YJ, Hamlin JL, Dutta A. Right place, right time, and only once: replication initiation in metazoans. Cell. 2005;123:13–24.
26. Qu K, Wang Z, Fan H, Li J, Liu J, Li P, et al. MCM7 promotes cancer progression through cyclin D1-dependent signaling and serves as a prognostic marker for patients with hepatocellular carcinoma. Cell Death Dis. 2017;8:e2603.
27. Mo L, Su B, Xu L, Hu Z, Li H, Du H, et al. MCM7 supports the stemness of bladder cancer stem-like cells by enhancing autophagic flux. iScience. 2022;25:105029.
28. Khvorova A. Modulation of DNA transcription: The future of ASO therapeutics? Cell. 2022;185:2011–3.
29. Crooke ST, Baker BF, Crooke RM, Liang X-H. Antisense technology: an overview and prospectus. Nat Rev Drug Discov. 2021;20:427–53.
30. Wang Z, Wang S, Qin J, Zhang X, Lu G, Liu H, et al. Splicing factor BUD31 promotes ovarian cancer progression through sustaining the expression of anti-apoptotic BCL2L12. Nat Commun. 2022;13:6246.

ACKNOWLEDGEMENTS

We thank American Journal Experts (AJE) for English language editing. Figdraw was used for image production.

AUTHOR CONTRIBUTIONS

Conception and design: YL, KS. Methodology: YL. Acquisition of data: YW, YL, ZC. Analysis and interpretation of data: YW, YL. Administrative, technical, or material support: YL, KS. Study supervision: YL, KS. Writing, review, and/or revision of the manuscript: YW, YL, KS. Final approval: All authors.

FUNDING

This work was supported by National Key Technology Research and Development Programme of China (2022YFC2704200 and 2022YFC2704202) and Natural Science Foundation of Shandong Province (ZR2023MH183).

COMPETING INTERESTS

The authors declare no competing interests.

ETHICS APPROVAL

Ethical approval was obtained from the Ethics Committee of Qilu Hospital, Shandong University (KYLL-202209-032).

ADDITIONAL INFORMATION

Supplementary information The online version contains supplementary material available at https://doi.org/10.1038/s41388-024-03015-2.

Correspondence and requests for materials should be addressed to Yingwei Li or Kun Song.